CMB spectral distortions from cooling macroscopic dark matter

Saurabh Kumar,[1,*] Emanuela Dimastrogiovanni,[1,2,†] Glenn D. Starkman,[1,‡] Craig Copi,[1,§] and Bryan Lynn[1,3,‖]
[1]*Department of Physics/CERCA/Institute for the Science of Origins, Case Western Reserve University, Cleveland, Ohio 44106-7079, USA*
[2]*Perimeter Institute for Theoretical Physics, 31 Caroline Street North, Waterloo, Ontario N2L 2Y5, Canada*
[3]*Department of Physics and Astronomy, University College London, Gower Street, London WC1E 6BT, United Kingdom*

(Received 3 May 2018; published 18 January 2019)

We propose a new mechanism by which dark matter (DM) can affect the early and late Universe. The hot interior of a *macroscopic* DM, or *macro*, can behave as a heat reservoir so that energetic photons and neutrinos are emitted from its surface and interior, respectively. In this paper, we focus on the spectral distortions (SDs) of the cosmic microwave background before recombination. The SDs depend on the density and the cooling processes of the interior and the surface composition of the macros. We use neutron stars as a model for nuclear-density macros and find that the spectral distortions are mass independent for a fixed density. In our work, we find that, for macros of this type that constitute 100% of the dark matter, the μ and y distortions can be near or above the detection threshold for typical proposed next-generation experiments such as PIXIE.

DOI: 10.1103/PhysRevD.99.023521

I. INTRODUCTION

In the standard ΛCDM model of cosmology, dark matter (DM) comprises $\Omega_{\rm DM} \sim 0.27$ of the total energy density of today's Universe. From observations of the cosmic microwave background (CMB) and cosmic structures, we know this DM must be "cold" (i.e., nonrelativistic) and "dark" (i.e., interact rarely with ordinary matter and radiation)—hence cold dark matter (CDM). It must also interact rarely with itself.

The microscopic nature of CDM is still unknown; however, the absence of a suitable Standard Model (SM) particle has driven the widespread belief that the DM is a beyond the Standard Model (BSM) particle and a concomitant decades-long search for such particles in purpose-built DM detectors and among the by-products of collisions at particle accelerators.

The ongoing infertility of such particle DM searches, whether for weakly interacting massive particles or axions, suggests that other candidates return to serious consideration. Two such candidates have long histories: so-called "primordial" black holes (PBHs) and composite baryonic objects of approximate nuclear density and macroscopic size, which we will refer to as "macros" [1], although that term properly includes macroscopic candidates of any density and composition.

This paper is focused on macros and, specifically, on observational consequences of the presence of nuclear-density macros in the early Universe. These have the particular virtue that they may be purely SM objects built of quarks or baryons. In this case, they must have been formed before the freeze-out of weak interactions at $t \simeq 1$ s and the subsequent onset of big bang nucleosynthesis (BBN), if the success of the standard theory of BBN in predicting light-element abundances is to be preserved (although see [2]).

Witten first suggested [3] that DM could be composites of up, down, and strange quarks assembled during the QCD phase transition. Subsequent proposals have included purely SM objects made of quarks [4] or baryons [5,6] of substantial average strangeness. A variety of BSM variations also exist (e.g., [7]). Several authors have focused on the observational consequences [1,8,9].

Macros share with PBHs an important distinction from particle DM candidates: They achieve their low interaction rates by being massive and, therefore, of much lower hypothetical number density. The nonobservation of approximately nuclear-density macros through the tracks they would have left in ancient mica [1] demands $m_X \gtrsim 55$ g. Limits on larger macro masses have been obtained from gravitational microlensing ($m_X \lesssim 2 \times 10^{20}$ g) [10–12] and femtolensing (excluding $10^{17} \lesssim m_X \lesssim 2 \times 10^{20}$ g). These limits as quoted assume that the DM consists of macros

*saurabh.kumar@case.edu
†exd191@case.edu
‡glenn.starkman@case.edu
§cjc5@case.edu
‖bryan.lynn@cern.ch

of a single mass—an unlikely situation for a composite object. Macroscopic bound states of fermions (e.g., quarks or baryons) cannot be formed by the gravitational collapse of adiabatic fluctuations in the radiation-dominated era. They would arise typically from nonadiabatic fluctuations [3,13] or topological defects [14] (e.g., from phase transitions) that enhance the fermion abundance relative to that of the radiation. Although there are stringent constraints on kaon or pion condensates, hyperons, and strange quark matter inside observed 2 $M_\odot$ or heavier neutron stars [15,16], these states may (or may not) be found in lighter neutron stars. Moreover, these exotic hadronic or quark matter equations of state are theoretically allowed; hence, one should not abandon the possibility of their playing a role in the structure of macros, which are certainly not the end points of ordinary stellar evolution. The mass functions of macros are model dependent and therefore difficult to predict [13]. We do not discuss further the origin of the macros but concern ourselves with their detection.

Cosmological constraints on macros, whether from the CMB or large-scale structure, do not yet impinge on generic nuclear-density objects.

The presence of dense assemblages of quarks or baryons from before BBN through today would undoubtedly have as-yet-unexplored observational consequences, no matter the specific mechanism of their formation or stabilization. Novel physics peculiar to such macros, with potential observational consequences, include:

(i) slow prerecombination cooling of the macro compared to the ambient plasma—
  (a) distorting the spectra of the cosmic microwave and neutrino backgrounds (CMB and CNB, respectively),
  (b) heating the postrecombination Universe, or
  (c) contributing to the cosmic infrared background;
(ii) production of nuclei (including heavy nuclei) through
  (a) inefficiency in macro assembly at formation,
  (b) evaporation, sublimation, or boiling, especially soon after macro formation, or
  (c) macro-macro collisions;
(iii) formation of binary macros, with potential gravitational-wave and electromagnetic signals;
(iv) DM self-interactions, especially in high-density environments such as galactic cores; and
(v) enhanced thermal and dynamical coupling of dark matter to baryons and photons.

These primary processes could have important secondary consequences, including implications for early star formation, assembly of supermassive black holes, and 21-cm emissions [17].

In this work, we focus our attention on the very first of these: the effect on the CMB and CNB of macroscopic objects that generically cool by volume emission of neutrinos and surface emission of photons. (BSM candidates may have additional cooling mechanisms.)

By considering a specific example of a baryonic macro—a neutron star (NS)—as a macro, we demonstrate that the weak coupling of neutrinos to baryons and the inefficiency of surface cooling by photons generically lead the macros to remain significantly hotter than the ambient plasma through the epoch of recombination. Both energy and entropy are therefore injected into the plasma in the form of photons and neutrinos well after the time when thermal or statistical equilibrium can be restored. The CMB and CNB spectra are thereby distorted.

In this first work, we characterize the distortion in terms of the traditional μ-type (photon-number excess) and y-type (photon-energy excess) spectral distortions (SDs) of the CMB and by $\Delta N_{\rm eff}$, the increase in the effective number of neutrino species. However, because the temperature of the macros can remain far above that of the ambient plasma, and because the cooling is ongoing through and after recombination, neither μ nor y will fully capture the shape of the resulting distortion. This will be considered in future work, as will the angular fluctuations in the distortion, its correlation with other observables, and other potential consequences of baryonic macro DM, as listed above.

The magnitude of SDs caused by macros is controlled, of course, by their abundance but also by their specific internal physics. For NS material, this includes the thickness and insulating properties of the nondegenerate crust; the equation of state of the neutrino-emitting core, in particular, the presence or absence of a superconducting phase, and its detailed properties.

For a solar-mass NS, known or anticipated properties result in μ- and y-type distortions of the CMB that are potentially above the threshold of detection by feasible next-generation SD experiments and $\Delta N_{\rm eff}$ that are not. These specific conclusions will change for other microphysical models of macros but may be instructive of what to expect and why. To our knowledge, this is the first study of the radiative cooling of DM and the CMB spectral distortions it may cause.

The CMB has been measured [18] to have a blackbody (BB) spectrum with an average temperature of 2.7255 ± 0.0006 K. Some deviation from a BB is predicted due to energy injection and absorption mechanisms [19–25], especially the damping of acoustic modes after they have entered the horizon, also known as Silk damping [19,22,26–33]. At very high redshifts, $z > z_\mu \equiv 2 \times 10^6$, distortions would be wiped out by an efficient photon number and energy-changing interactions. For $5 \times 10^4 \lesssim z \lesssim 2 \times 10^6$, number-changing mechanisms are inefficient, and photon injection results in a finite chemical potential in the Bose-Einstein distribution of photons, a so-called μ distortion. At lower redshifts, $z \lesssim 5 \times 10^4$, energy redistribution by Compton scattering becomes inefficient, leading to y-type distortions. The intermediate era, $z \approx 10^4$–10^5, is also characterized by *i-type* distortions [34].

The only macroscopic objects of nuclear density known to exist in nature are NSs formed as end points of stellar evolution. These appear to have masses below $2.2\,M_\odot$ [35,36], well below the total mass within the horizon at $z \sim 10^9$ (or even 10^{12}, the epoch of quark confinement and chiral symmetry breaking). We therefore use an ordinary NS as a proxy for a macro. We take the macro's central density to be $\rho_X \simeq \rho_N \equiv 2.8 \times 10^{14}\ \mathrm{g/cm^3}$, which we refer to as the nuclear density. Although microlensing limits preclude all the DM being NSs, the macro mass function could include a sizable contribution from them.

Neutron stars theoretically are stable down to $(0.09\text{–}0.19)M_\odot$ [37–40] but do not appear to arise as the end points of the evolution of main-sequence stars below $\sim 1.2\ M_\odot$. If formed in the early Universe, these would be larger and of lower average density than poststellar neutron stars. This motivates us to consider NS-like macros of somewhat lower-than-nuclear density.

The discovery of a NS with $M_{\rm NS} < 1.2\ M_\odot$ would be exciting evidence for early-Universe macro formation.

Smaller-still composite baryonic objects require nongravitational stabilization, whether within the SM through the incorporation of strange quarks or baryons [3,5,6] or by more exotic BSM mechanisms. Such SM or BSM baryonic composites may also exist in the mass range that includes stable NSs.

The paper is organized as follows. In Sec. II, we discuss the neutrino and photon emission processes that cool the macro. In Sec. III, we calculate the SD created by photon emission from the surface of macros. In Sec. IV, we present our conclusions. We provide a derivation for the photon luminosity of the macro and describe the neutrino cooling processes in more detail in the Appendixes.

II. COOLING OF MACROS

In this section, we provide expressions for the neutrino and photon luminosities from the interior and surface of the macro, respectively. We then arrive at the temperature dependence of the interior of the macro.

Except for the inner core, the composition of which is still under debate, a NS is composed of neutrons, protons, electrons, and heavy ions. After formation, it cools down via neutrino emission from the interior and photon emission from the surface.

Neutrino cooling occurs through three processes: (i) direct Urca (DUrca)

$$n \to p + e^- + \bar{\nu}_e, \qquad e^- + p \to n + \nu_e$$

takes place at high temperatures, when neutrons and electrons are nondegenerate, but may also be important below the degeneracy temperature; (ii) modified Urca (MUrca) in the neutron and proton branches

$$n + n \to n + p + e^- + \bar{\nu}_e, \quad n + e^- + p \to n + n + \nu_e,$$
$$n + p \to p + p + e^- + \bar{\nu}_e, \quad p + e^- + p \to n + p + \nu_e$$

is dominant at $T < 10^9$ K, when neutrons and electrons are degenerate; (iii) nucleon Cooper pair (CP) cooling

$$\tilde{N} + \tilde{N} \to \mathrm{CP} + \nu + \bar{\nu}$$

(where $\tilde{N}$ is a quasinucleon) is most efficient for $0.98T_c \gtrsim T \gtrsim 0.2T_c$, with neutrons in the NS interior become superconducting at T_c [41].

The luminosity of these neutrino-cooling processes is

$$\mathcal{L}_\nu^i = 10^{45} C_i (M_X/M_\odot)(\rho_X/\rho_N)^{-1/3}\ \mathrm{erg/s} \qquad (1)$$

for $i = \mathrm{DU, MU, CP}$. M_X is the mass of the macro. ρ_X is the density of the core, and it partly characterizes our ignorance of the precise properties of the macro. T dependence is encoded in

$$C_i = \begin{cases} 5.2 (T_9^X)^6 R^D & i = \mathrm{DU} \\ (3.0 R_n^M + 2.4 R_p^M) 10^{-6} (T_9^X)^8 \alpha & i = \mathrm{MU} \\ 7.1 \times 10^{-6} (\rho_X/\rho_N)^{-1/3} (T_9^X)^7 a F & i = \mathrm{CP}. \end{cases}$$

T^X is the macro's internal temperature; the subscript 9 will be used for a temperature in units of 10^9 K. In the above equation, $\alpha \simeq 2(1 + m_\pi^2/p_F^2(n))^{-2} - 0.3(1 + m_\pi^2/p_F^2(n))^{-1} + 0.07$, where $p_F(n) = 340(\rho_X/\rho_N)^{1/3}\ \mathrm{MeV}/c$ is the neutrons' Fermi momentum; R^D, R_n^M, and $R_p^M \le 1$ are reduction factors due to superfluidity [42,43]; a [44] and F [45] are the dimensionless factor and the control function, respectively, both of which depend on the type of superfluidity. The factors in the above expressions which depend on superfluidity have been discussed briefly in Appendix B.

The macro photon luminosity is

$$\mathcal{L}_\gamma = 10^{45} \left(\frac{M_X/\rho_X}{M_\odot/\rho_N} \right)^{2/3} (T_9^{s\,4} - T_9^{\mathrm{CMB}\,4})\ \mathrm{erg/s}, \qquad (2)$$

where T^s is the surface temperature of the macro and T^{CMB} is the temperature of the ambient plasma.

We assume that the macros have coalesced, and we can begin following their cooling from when the temperature of the ambient plasma is 10^9 K, at $z = 3.7 \times 10^8$. (This is after any electroweak and QCD-associated phase transitions [13].) We take the macro to be isothermal at that moment with the temperature equal to that of the plasma. The interior electrons, neutrons, and protons will be degenerate. The cooling of neutron stars below this temperature has been well explored, and we have verified that our conclusions are insensitive to the details of the macro cooling before this epoch.

We assume that the macro, like a NS, has a degenerate isothermal interior containing neutrons, protons, and

electrons and a nondegenerate "atmosphere" of electrons and heavy ions. This keeps the interior warm as the ambient plasma cools. For constant atmospheric photon luminosity $\mathcal{L}_\gamma$, the atmospheric density and temperature are related by

$$\rho_{\rm atm} = 1.2\times 10^{10}\rho_N \left(\frac{\mu(M_X/M_\odot)\ {\rm erg/s}}{Z(1+W)\mathcal{L}_\gamma}\right)^{1/2} T_9^{3.25}, \tag{3}$$

where μ, Z, and W are the mean molecular weight, metallicity or mass fraction of elements heavier than hydrogen and helium, and mass fraction of hydrogen, respectively. In case of a low-metallicity atmosphere, the Kramer's opacity due to bound-free transitions assumed above will be exceeded by the opacity due to free-free transitions, which does not vanish for low metallicity. This means Eq. (3) will not diverge for small Z.

Where the atmosphere meets the interior, the relation between density ρ_* and temperature T^* can be found (see [46], Chap. 4) by equating the electron pressure of the degenerate interior and the nondegenerate atmosphere

$$\rho_* = 7.6\times 10^5 \mu_e T_9^{*3/2}\ {\rm g/cm^3}, \tag{4}$$

where μ_e is the mean molecular weight per electron. Equating (3) and (4),

$$\mathcal{L}_\gamma = 8.9\times 10^{36}\lambda(M_X/M_\odot)T_9^{*3.5}\ {\rm erg/s}, \tag{5}$$

where $\lambda \equiv (\frac{\mu}{\mu_e^2})\frac{2.0}{Z(1+W)}$. In the case of a NS, $\lambda \approx 1$ (see [46], Chap. 11). We take λ to be a free parameter that, along with ρ_X, represents the unknown characteristics of the macros. We provide a brief derivation of the photon luminosity in Appendix A.

The macro interior is nearly isothermal, due to the thermal conductivity of the degenerate electrons. Since $T^X \simeq T^*$, equating the photon luminosity (2) at the surface to (5) yields the macro's surface temperature $T_9^s(t)$.

Starting from its assumed initial isothermal condition at 10^9 K, the macro cools according to

$$\frac{dU_X}{dt} = -(\mathcal{L}_\nu^{\rm DU} + \mathcal{L}_\nu^{\rm MU} + \mathcal{L}_\nu^{\rm CP} + \mathcal{L}_\gamma), \tag{6}$$

where the internal energy is [see [46], Eq. (11.8.2)]

$$U_X = 6.1\times 10^{47}(M_X/M_\odot)(\rho_X/\rho_N)^{-2/3}T_9^{X2}\ {\rm erg}. \tag{7}$$

We refer the reader to Appendix A for a derivation of the above equation.

The interior temperature of the macro therefore obeys

$$\frac{d}{dt}T_9^X = -8.3\times 10^{-4}\ {\rm s^{-1}}(\rho_X/\rho_N)^{1/3}T_9^{X-1}\sum_i C_i, \tag{8}$$

where the sum over i now includes photons and $C_\gamma \equiv 8.9\times 10^{-9}(\rho_X/\rho_N)^{1/3}\lambda(T_9^X)^{7/2}$.

Neutrino emission via MUrca occurs from the onset, since we take the initial temperature to be 10^9 K. Emission via CP begins below T_{c9}. We explore two possibilities: first, no DUrca cooling $R^D = 0$; second, a proton fraction sufficient to support DUrca, with R^D given by Eq. (19) in Ref. [42].

In practice, SDs are relatively insensitive to the exact values of these various numerical factors.

In the case where there is negligible DUrca emission, cooling proceeds in three stages: *stage 1.*—MUrca-dominated cooling from $T_9^X = T_9^{\rm MU} = 1$, at time t_9, to $T_9^{\rm CP} = 0.98T_{c9}$, at t_{CP}; *stage 2.*—CP-dominated cooling from $T_9^{\rm CP}$ to $T_9^\gamma \simeq 0.2T_{c9}$ at t_γ; *stage 3.*—photon cooling below T_9^γ, i.e., after t_γ. (If T_9^{CP} is high enough, the first stage may be omitted.) The macro cooling can be followed numerically, but, by assuming that the dominant cooling mechanism in each stage is the only one (and taking $R_n^M, R_p^M = 1$), we find

$$T_9^X(t) \simeq \begin{cases} T_9^{\rm MU}\left[1+2.7\times 10^{-8}\alpha T_9^{\rm MU6}\left(\frac{\rho_X}{\rho_N}\right)^{1/3}\frac{t-t_9}{s}\right]^{-1/6} \\ \text{for } 1 \equiv T_9^{\rm MU} \geq T_9^X \geq T_9^{\rm CP} \simeq 0.98T_{c9}, \\ T_9^{\rm CP}\left[1+1.8\times 10^{-2}aFT_9^{\rm CP5}\frac{t-t_{\rm CP}}{s}\right]^{-1/5} \\ \text{for } 0.98T_{c9} \simeq T_9^{\rm CP} \geq T_9^X \geq T_9^\gamma \simeq 0.2T_{c9}, \\ T_9^\gamma\left[1.0+1.1\times 10^{-11}\lambda T_9^{\gamma 3/2}(\rho_X/\rho_N)^{2/3}\frac{t-t_\gamma}{s}\right]^{-2/3} \\ \text{for } 0.2T_{c9} \simeq T_9^\gamma \geq T_9^X. \end{cases} \tag{9}$$

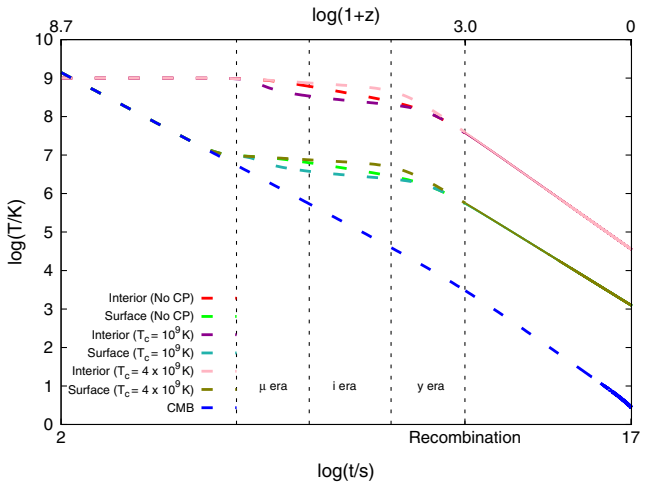

FIG. 1. Interior temperature T_X and surface temperature T_s of a macro for $M_X = M_\odot$, $\lambda = 1$, and $\rho_X = \rho_N$, plotted vs time t and redshift z. Cooling is without DUrca and both without CP and with CP for two values of T_c. The ambient photon temperature $T_{\rm CMB}$ is shown for a comparison, and the eras when μ and y distortions occur are indicated.

TABLE I. Definitions of various temperatures, T_9^i, that appear in Eqs. (9) and (10). For $i = \mathrm{MU}, \mathrm{DU}, CP$, the temperature values were determined by comparing the luminosities of various processes given by Eq. (1).

	Description
T_9^X	Interior temperature of macro
T_9^{CMB}	CMB temperature
T_9^{MU}	Temperature of macro at onset of MUrca
T_9^{DU}	Temperature of macro at onset of DUrca
T_9^{CP}	Temperature of macro at onset of CP cooling

TABLE II. Definitions of various times t_i, that appear in Eqs. (9) and (10). These time values were obtained by solving Eq. (9) for the most dominant cooling process.

	Description
t_9	Cosmic time at which $T_9^X = 1$
t_{CP}	Cosmic time at which CP cooling dominates
t_γ	Cosmic time at which photon cooling dominates

The above relations can also be expressed in terms of redshift z, using the time-redshift relation $z = 4.9 \times 10^9 (t/\mathrm{s})^{-1/2}$. The times (and thus redshifts) at which the interior temperature T_X falls to T_γ depend on detailed properties of the macro, such as its central density ρ_X and the composition parameter λ. In Fig. 1, we plot the central and surface temperatures of the macro, as well as the CMB temperature as a function of the time for a representative value of these parameters.

In the presence of DUrca cooling, stage 1 is DUrca dominated until T_9^X becomes $T_9^\gamma = 0.1 T_{c9}$ at t_γ. In this case, during stage 1 (now $T_9^{\mathrm{DU}} \equiv 1$)

$$T_9^X(t) = T_9^{\mathrm{DU}} \left[1 + 0.017 (T_9^{\mathrm{DU}})^4 R^D \left(\frac{\rho_X}{\rho_N} \right)^{1/3} \frac{t - t_9}{s} \right]^{-1/4}. \tag{10}$$

For convenience, we provide Tables I and II, where we describe the various temperatures and times that appear in Eqs. (9) and (10).

III. SPECTRAL DISTORTIONS BY MACROS

The prerecombination contributions to μ and y distortions of the CMB can be approximated by

$$\begin{Bmatrix} \mu \\ y \end{Bmatrix} = \int dt \mathcal{J}_{\mathrm{bb}} \begin{Bmatrix} 1.4 \mathcal{J}_\mu \\ \frac{1}{4} \mathcal{J}_y \end{Bmatrix} \frac{1}{c^2 \rho_\gamma} \dot{Q}. \tag{11}$$

The window functions given in Refs. [22,47,48] are

$$\mathcal{J}_y(z) = 1 - \mathcal{J}_\mu(z) \approx [1 + 4.7 \times 10^{-13} z^{2.58}]^{-1},$$
$$\mathcal{J}_{\mathrm{bb}}(z) \approx \exp[-(z/z_\mu)^{5/2}]. \tag{12}$$

The CMB energy density $\rho_\gamma \approx 7.0 \times 10^{-34} z(t)^4$ g/cm^3, while the rate at which energy density is injected into the photon distribution by macros of density n_X is

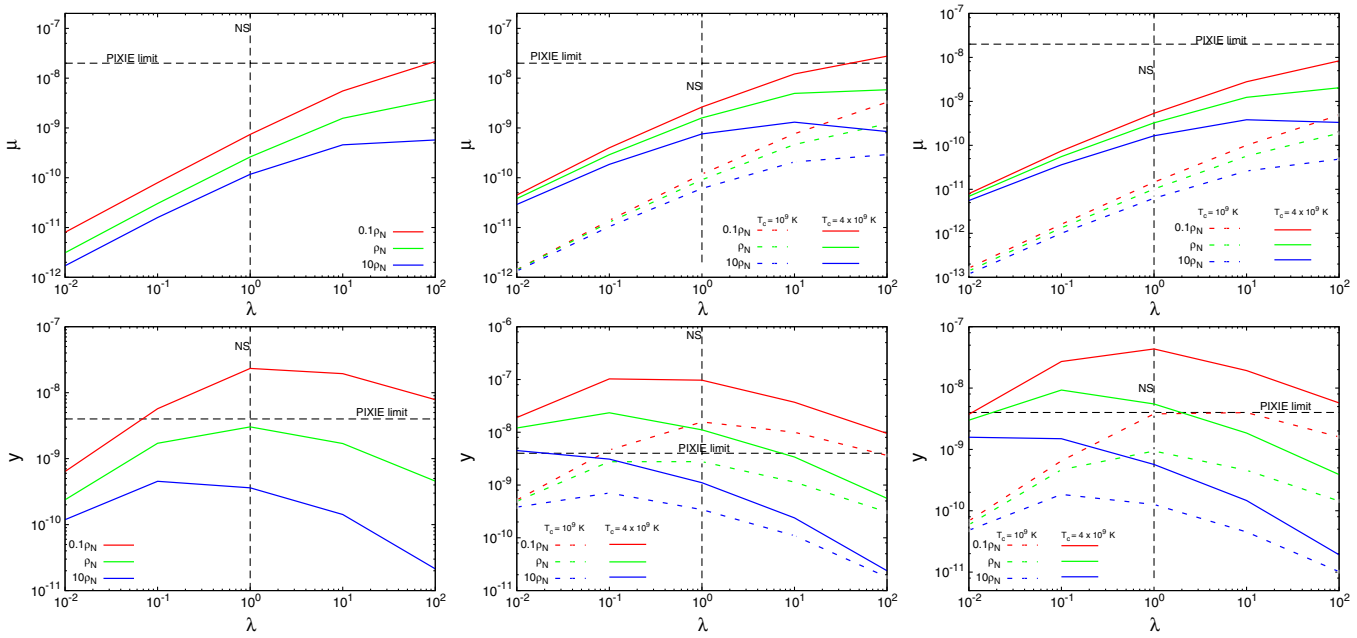

FIG. 2. Top panel: μ distortion as a function of macro surface composition factor λ for three different cooling scenarios. On the left, no DUrca, no CP; in the middle, no DUrca, with CP; on the right, with DUrca, with CP. Green lines denote $\rho_X = \rho_N$, red lines $0.1\rho_N$, and blue lines $10\rho_N$. The panels with CP show results for $T_c = 10^9$ K (dashed lines) and $T_c = 4 \times 10^9$ K (solid lines). Bottom panel: As for the top panel but for y distortion. The vertical dashed line stands for $\lambda = 1$, which is similar to a neutron star.

$$\dot{Q} = n_X \mathcal{L}_\gamma. \tag{13}$$

It is useful to rewrite $n_X = \Omega_{X0}\rho_c z(t)^3/M_X$ with $\rho_c \simeq 10^{-29}$ g/cm^3 and macro DM fraction $\Omega_{X0} \lesssim 0.24$.

In Fig. 2, we plot μ and y (obtained numerically) vs λ for $M_X = M_\odot$, macro densities near the fiducial ρ_N, and a variety of cooling scenarios.

We have also calculated the perturbation to the neutrino energy density, since neutrinos are injected well after weak-interaction freeze-out at $T_{\rm CMB9} \simeq 10$, but the change in $N_{\rm eff}$ is negligible. This could change if the internal physics of the macro were radically different.

The predicted y distortion is comparable to the target sensitivities of anticipated next-generation spectral distortion satellite missions, and the predicted μ distortion is nearly so. We remind the reader that, since macros are much hotter than the plasma through much of their history and stay hot well after recombination, μ and y do not adequately capture the detectability of the SD signal.

Although we have presented results for $M_X = M_\odot$, the spectral distortions μ and y are mass independent, for fixed ρ_X, since $\mathcal{L}_\gamma \propto M_X$ from (5), while $n_X \propto M_X^{-1}$, and so $\dot{Q} \propto M_X^0$. The distortions will however depend on ρ_X, as well as on the detailed physics of the surface layer (as parametrized by λ), and the cooling mechanisms operative in an actual macro.

IV. CONCLUSIONS

We have demonstrated that the presence of macroscopic DM in the early Universe may lead to observable signatures in the CMB spectrum. To fully characterize these distortions, the full spectral distortion must be inferred numerically using the Boltzmann equation—this includes so-called intermediate distortions, a more complete characterization of the distorted spectrum, and continued contributions to the distortions postrecombination. Also, the temperature of macros postrecombination may stay much higher compared to the CMB for an extended period, implying the presence of hot relics that could be visible as an associated background radiation or could heat the postrecombination Universe.

Other signatures can also be anticipated, such as correlations between CMB temperature anisotropies and spectral distortion anisotropies, the presence of heavy elements in the prerecombination Universe, and the continued production of these elements postrecombination and outside stars. The unexplored possibilities for observable consequences of Standard Model DM are yet rich.

ACKNOWLEDGMENTS

S. K., G. D. S., and B. L. are partially supported by U.S. Department of Energy Grant No. DE-SC0009946.

APPENDIX A: PHOTON LUMINOSITY AND INTERNAL TEMPERATURE OF MACRO

In this Appendix, we derive the temperature dependence of the Macro given by Eq. (8), following closely the treatment of Chap. 4 in Ref. [46].

We assume that below the degeneracy temperature of 10^9 K, the core of the macro is composed of degenerate neutron-proton-electron plasma and is isothermal. The atmosphere is composed of a nondegenerate layer. The energy transfer due to photon diffusion from the hot interior to the ambient CMB through the atmosphere can be described by the radiative heat transfer equation assuming local thermal equilibrium and the steady state. The photon luminosity $\mathcal{L}_\gamma$ is given by

$$\mathcal{L}_\gamma = -4\pi r^2 \frac{c}{3\kappa\rho_{\rm atm}} \frac{d}{dr}(aT^4), \tag{A1}$$

where a is the radiation constant, r is the radial distance from the center of the macro, and κ, $\rho_{\rm atm}$, and T are the Rosseland mean opacity, the density, and the temperature of the atmosphere, respectively.

Opacity κ can be approximated as Kramer's opacity:

$$\kappa = \kappa_0 \rho_{\rm atm} T^{-3.5}, \tag{A2}$$

where

$$\kappa_0 = 4.34 \times 10^{24} Z(1+X)\ {\rm cm}^2\,{\rm g}^{-1}. \tag{A3}$$

Hydrostatic equilibrium requires that the pressure of the atmosphere depends on the radius as

$$\frac{dP}{dr} = -\frac{Gm(r)\rho_{\rm atm}}{r^2}, \tag{A4}$$

where $m(r)$ is the mass of the macro within the radius r. Since the atmosphere is much thinner than the radius of the core, we can set $m(r) = M_X$.

The pressure for a nondegenerate gas is also given by the ideal gas law:

$$P(r) = \frac{\rho_{\rm atm}}{\mu m_u} k_B T, \tag{A5}$$

where μm_u is the mean molecular weight. (m_u is the atomic mass unit.)

Substituting (A5) in (A4), and using (A2) and (A1),

$$PdP = 5.33ac \frac{\pi G M_X}{\kappa_0 \mathcal{L}_\gamma} \frac{k_B}{\mu m_u} T^{7.5} dT. \tag{A6}$$

Assuming a constant luminosity throughout the thin atmosphere, we can integrate the above equation with the boundary condition, $P = 0$ when $T = 0$. Thus, we arrive at the density of the atmosphere given by Eq. (3):

$$\rho_{\rm atm} = \sqrt{1.25ac\frac{\pi GM}{\kappa_0\mathcal{L}_\gamma}\frac{\mu m_u}{k_B}T^{3.25}}$$
$$= 1.2\times10^{10}\rho_N\left(\frac{\mu(M_X/M_\odot)\ \text{erg/s}}{Z(1+W)\mathcal{L}_\gamma}\right)^{1/2}T_9^{3.25}. \quad \text{(A7)}$$

At the point where the atmosphere meets the core, the nondegenerate electron pressure of the atmosphere given by the ideal gas law is equal to the electron degeneracy pressure of the core:

$$\frac{\rho_* k_B T_*}{\mu_e m_u} = 1.0\times10^{13}\left(\frac{\rho_*}{\mu_e}\right)^{5/3}, \quad \text{(A8)}$$

where μ_e is the mean molecular weight per electron and ρ_* and T_* are the density and temperature, respectively, at this transition point. Solving for ρ_* in the above equation and equating it with (A7), we get the luminosity of the macro given by Eq. (5):

$$\mathcal{L}_\gamma = (5.7\times10^5\ \text{erg/s})\frac{\mu}{\mu_e^2}\frac{1}{Z(1+W)}\frac{M_X}{M_\odot}T_*^{3.5}$$
$$= (8.9\times10^{36}\ \text{erg/s})\lambda(M_X/M_\odot)T_9^{*3.5}. \quad \text{(A9)}$$

From Ref. [49], the heat capacity of the macro at temperature T_X is

$$C_v = \left.\frac{dU_X}{dT_X}\right|_{N,V} = \frac{\pi^2(x^2+1)^{1/2}}{x^2}Nk_B\left(\frac{k_BT_X}{mc^2}\right), \quad \text{(A10)}$$

where U_X, N, and V are the internal energy, total number of neutrons, and volume of the macro, respectively. In the above equation, $x = p_f/m_nc$ is the relativity parameter, where p_f is the Fermi momentum and m_n is the mass of the neutron. Integrating the above equation over T_X gives us Eq. (7) for the internal energy:

$$U_X = (6.1\times10^{47}\ \text{erg})\left(\frac{M_X}{M_\odot}\right)\left(\frac{\rho_X}{\rho_N}\right)^{-2/3}(T_9^X)^2. \quad \text{(A11)}$$

We can use this expression for U_X in the left-hand side of Eq. (6). The right-hand side of Eq. (6) is a sum of the photon luminosity (A9) and neutrino luminosities that we will briefly describe in the Appendix below.

APPENDIX B: NEUTRINO EMISSION LUMINOSITY

In this Appendix, we describe briefly the neutrino emissions from the macro as given by Eq. (1). A detailed derivation of (1) is beyond the scope of this paper. Moreover, the expressions for the luminosities are very well established and have been studied in great detail [42,43,45].

The DUrca luminosity [42]

$$\mathcal{L}_\nu^{\rm DU} = 5.2\times10^{45}(T_9^X)^6R^D\left(\frac{M_X}{M_\odot}\right)\left(\frac{\rho_X}{\rho_N}\right)^{-1/3}\text{erg/s}, \quad \text{(B1)}$$

where R^D is the reduction factor in DUrca rate due to superfluidity. As an example, we considered the type-AA superfluidity of neutrons and protons. The R^D is given by Eq. (19) in Ref. [42]:

$$R^D = \frac{u}{u+0.9163}S + D,$$
$$S = \frac{1}{I_0}(K_0+K_1+0.42232K_2)\left(\frac{\pi}{2}\right)^{1/2}p_s^{1/4}e^{-\sqrt{p_e}},$$
$$I_0 = 457\pi^6/5040,$$
$$K_0 = \frac{\sqrt{p-q}}{120}(6p^2+83pq+16q^2)$$
$$-\sqrt{p}\frac{q}{8}(4p+3q)\ln\left(\frac{\sqrt{p}+\sqrt{p-q}}{\sqrt{q}}\right),$$
$$K_1 = \frac{\pi^2\sqrt{p-q}}{6}(p+2q) - \frac{\pi^2}{2}q\sqrt{p}\ln\left(\frac{\sqrt{p}+\sqrt{p-q}}{\sqrt{q}}\right),$$
$$K_2 = \frac{7\pi^4}{60}\sqrt{p-q},$$
$$2p = u+12.421+\sqrt{w^2+12.350u+45.171},$$
$$2q = u+12.421-\sqrt{w^2+12.350u+45.171},$$
$$2p_s = u+\sqrt{w^2+5524.8u+6.7737},$$
$$2p_e = u+0.43847+\sqrt{w^2+8.3680u+491.32},$$
$$D = 1.52(u_1u_2)^{3/2}(u_1^2+u_2^2)e^{-u_1-u_2},$$
$$u_1 = 1.8091+\sqrt{v_1^2+(2.2476)^2},$$
$$u_2 = 1.8091+\sqrt{v_2^2+(2.2476)^2},$$
$$u = v_1^2+v_2^2,$$
$$w = v_2^2-v_1^2,$$
$$v_1 = v_2 = v_A = \sqrt{1-\tau}\left(1.456-\frac{0.157}{\sqrt{\tau}}+\frac{1.764}{\tau}\right), \quad \text{(B2)}$$

where

$$\tau \equiv \frac{T_X}{T_c}. \quad \text{(B3)}$$

The MUrca luminosity [43]

$$\mathcal{L}_\nu^{\rm MU} = (3.0R_n^M+2.4R_p^M)10^{39}(T_9^X)^8\alpha$$
$$\times(M_X/M_\odot)(\rho_X/\rho_N)^{-1/3}\ \text{erg/s}. \quad \text{(B4)}$$

For simplicity, we consider only singlet-state neutron superfluidity of type **A**. The associated reduction factors R_n^M and R_p^M are given by Eqs. (32) and (37) in Ref. [43]:

$$R_n^M = \frac{a^{7.5}+b^{5.5}}{2} e^{3.4370-\sqrt{(3.4370)^2+v^2}},$$
$$a = 0.1477 + \sqrt{(0.8523)^2+(0.1175v)^2},$$
$$b = 0.1477 + \sqrt{(0.8523)^2+(0.1297v)^2},$$
$$v = \sqrt{1-\tau}\left(1.456 - \frac{0.157}{\sqrt{\tau}} + \frac{1.764}{\tau}\right),$$

and

$$R_p^M = \left(0.2414 + \sqrt{(0.7586)^2+(0.1318v)^2}\right)^7 e^{5.339-\sqrt{(5.339)^2+(2v)^2}}, \quad \text{(B5)}$$

respectively.

The *CP* cooling luminosity [45]

$$\mathcal{L}_\nu^{\rm CP} = 7.1\times 10^{39}\ {\rm erg/s}(T_9^X)^7 aF \times (M_X/M_\odot)(\rho_X/\rho_N)^{-2/3}\ {\rm erg/s}. \quad \text{(B6)}$$

The function F controls the efficiency of the *CP* cooling process. We select F to be F_A given by

$$F_A(v) = (0.602v^2+0.5942v^4+0.288v^6) \times \left(0.5547+\sqrt{(0.4453)^2+0.01130v^2}\right)^{1/2} \times e^{-\sqrt{4v^2+(2.245)^2}+2.245}, \quad \text{(B7)}$$

Eq. (34) in Ref. [45]. The factor a in the *CP* luminosity is a constant that depends on the nucleon species and superfluidity type. It has the maximum value of 4.17 and 3.18 for triplet states of neutrons and protons, respectively.

[1] D. M. Jacobs, G. D. Starkman, and B. W. Lynn, Mon. Not. R. Astron. Soc. **450**, 3418 (2015).
[2] S. Dimopoulos, R. Esmailzadeh, L. J. Hall, and G. D. Starkman, Astrophys. J. **330**, 545 (1988).
[3] E. Witten, Phys. Rev. D **30**, 272 (1984).
[4] E. Farhi and R. L. Jaffe, Phys. Rev. D **30**, 2379 (1984).
[5] B. W. Lynn, A. E. Nelson, and N. Tetradis, Nucl. Phys. **B345**, 186 (1990).
[6] B. W. Lynn, arXiv:1005.2124.
[7] A. R. Zhitnitsky, Nucl. Phys. B, Proc. Suppl. **124**, 99 (2003).
[8] A. De Rújula and S. Glashow, Nature (London) **312**, 734 (1984).
[9] J. Rafelski, L. Labun, and J. Birrell, Phys. Rev. Lett. **110**, 111102 (2013).
[10] M. Zumalacarregui and U. Seljak, Phys. Rev. Lett. **121**, 141101 (2018).
[11] K. Griest, A. M. Cieplak, and M. J. Lehner, Phys. Rev. Lett. **111**, 181302 (2013).
[12] H. Niikura *et al.*, arXiv:1701.02151.
[13] A. E. Nelson, Phys. Lett. B **240**, 179 (1990).
[14] X. Liang and A. Zhitnitsky, Phys. Rev. D **94**, 083502 (2016).
[15] J. M. Lattimer, Annu. Rev. Nucl. Part. Sci. **62**, 485 (2012).
[16] J. M. Lattimer and M. Prakash, Astrophys. J. **550**, 426 (2001).
[17] A. Fialkov (private communication).
[18] J. C. Mather *et al.*, Astrophys. J. **420**, 439 (1994).
[19] J. D. Barrow and P. Coles, Mon. Not. R. Astron. Soc. **248**, 52 (1991).
[20] R. Khatri, R. A. Sunyaev, and J. Chluba, Astron. Astrophys. **540**, A124 (2012).
[21] Y. B. Zeldovich and R. A. Sunyaev, Astrophys. Space Sci. **4**, 301 (1969).
[22] R. A. Sunyaev and Y. B. Zeldovich, Astrophys. Space Sci. **7**, 3 (1970).
[23] L. Danese and G. de Zotti, Nuovo Cimento Riv. Ser. **7**, 277 (1977).
[24] W. Hu and J. Silk, Phys. Rev. D **48**, 485 (1993).
[25] J. Chluba and R. A. Sunyaev, Mon. Not. R. Astron. Soc. **419**, 1294 (2012).
[26] R. A. Daly, Astrophys. J. **371**, 14 (1991).
[27] W. Hu, D. Scott, and J. Silk, Astrophys. J. **430**, L5 (1994).
[28] J. Chluba, R. Khatri, and R. A. Sunyaev, Mon. Not. R. Astron. Soc. **425**, 1129 (2012).
[29] E. Pajer and M. Zaldarriaga, Phys. Rev. Lett. **109**, 021302 (2012).
[30] J. Chluba, A. L. Erickcek, and I. Ben-Dayan, Astrophys. J. **758**, 76 (2012).
[31] R. Emami, E. Dimastrogiovanni, J. Chluba, and M. Kamionkowski, Phys. Rev. D **91**, 123531 (2015).
[32] E. Dimastrogiovanni and R. Emami, J. Cosmol. Astropart. Phys. 12 (2016) 015.
[33] J. Chluba, E. Dimastrogiovanni, M. A. Amin, and M. Kamionkowski, Mon. Not. R. Astron. Soc. **466**, 2390 (2017).
[34] R. Khatri and R. A. Sunyaev, J. Cosmol. Astropart. Phys. 09 (2012) 016.
[35] B. Margalit and B. D. Metzger, Astrophys. J. **850**, L19 (2017).
[36] J. Alsing, H. O. Silva, and E. Berti, Mon. Not. R. Astron. Soc. **478**, 1377 (2018).
[37] M. Colpi, S. L. Shapiro, and S. A. Teukolsky, Astrophys. J. **414**, 717 (1993).
[38] G. H. Bordbar and M. Hayati, Int. J. Mod. Phys. A **21**, 1555 (2006).
[39] A. Y. Potekhin, A. F. Fantina, N. Chamel, J. M. Pearson, and S. Goriely, Astron. Astrophys. **560**, A48 (2013).

[40] R. Belvedere, K. Boshkayev, J. A. Rueda, and R. Ruffini, Nucl. Phys. **A921**, 33 (2014).
[41] D. G. Yakovlev, K. P. Levenfish, and Y. A. Shibanov, Phys. Usp. **42**, 737 (1999).
[42] K. P. Levenfish and D. G. Yakovlev, Astron. Lett. **20**, 43 (1994).
[43] D. Yakovlev and K. Levenfish, Astron. Astrophys. **297**, 717 (1995).
[44] D. Page, J. M. Lattimer, M. Prakash, and A. W. Steiner, Astrophys. J. **707**, 1131 (2009).
[45] D. G. Yakovlev, A. D. Kaminker, and K. P. Levenfish, Astron. Astrophys. **343**, 650 (1999).
[46] S. Shapiro and S. Teukolsky, *Black Holes, White Dwarfs, and Neutron Stars* (Wiley-Interscience, New York, 1983).
[47] L. Danese and G. de Zotti, Astron. Astrophys. **107**, 39 (1982).
[48] R. Khatri and R. A. Sunyaev, J. Cosmol. Astropart. Phys. 06 (2012) 038.
[49] S. Chandrasekhar, *An introduction to the study of stellar structure* (University of Chicago, Chicago, 1939).